1521-0103/356/2/354–365$25.00
THE JOURNAL OF PHARMACOLOGY AND EXPERIMENTAL THERAPEUTICS

http://dx.doi.org/10.1124/jpet.115.230052
J Pharmacol Exp Ther 356:354–365, February 2016

Dinaciclib, a Cyclin-Dependent Kinase Inhibitor Promotes Proteasomal Degradation of Mcl-1 and Enhances ABT-737–Mediated Cell Death in Malignant Human Glioma Cell Lines[S]

Esther P. Jane, Daniel R. Premkumar, Jonathon M. Cavaleri, Philip A. Sutera, Thatchana Rajasekar, and Ian F. Pollack

Department of Neurologic Surgery, Children's Hospital of Pittsburgh (E.P.J., D.R.P., I.F.P.), University of Pittsburgh, School of Medicine (E.P.J., D.R.P., J.M.C., P.A.S., T.R., I.F.P), and University of Pittsburgh Brain Tumor Center (D.R.P., I.F.P.), Pittsburgh, Pennsylvania

Received October 15, 2015; accepted November 17, 2014

ABSTRACT

The prognosis for malignant glioma, the most common brain tumor, is still poor, underscoring the need to develop novel treatment strategies. Because glioma cells commonly exhibit genomic alterations involving genes that regulate cell-cycle control, there is a strong rationale for examining the potential efficacy of strategies to counteract this process. In this study, we examined the antiproliferative effects of the cyclin-dependent kinase inhibitor dinaciclib in malignant human glioma cell lines, with intact, deleted, or mutated p53 or phosphatase and tensin homolog on chromosome 10; intact or deleted or p14ARF or wild-type or amplified epidermal growth factor receptor. Dinaciclib inhibited cell proliferation and induced cell-cycle arrest at the G2/M checkpoint, independent of p53 mutational status. In a standard 72-hour 3-[4,5-dimethylthiazol- 2yl]-5-[3-carboxymethoxyphenyl]-2-[4-sulfophenyl]-2H, tetrazolium (MTS) assay, at clinically relevant concentrations, dose-dependent antiproliferative effects were observed, but cell death was not induced. Moreover, the combination of conventional chemotherapeutic agents and various growth-signaling inhibitors with dinaciclib did not yield synergistic cytotoxicity. In contrast, combination of the Bcl-2/Bcl-xL inhibitors ABT-263 (4-[4-[[2-(4-chlorophenyl)-5,5-dimethylcyclohexen-1-yl]methyl] piperazin-1-yl]-N-[4-[[(2R)-4-morpholin-4-yl-1-phenylsulfanylbutan-2-yl]amino]-3-(trifluoromethylsulfonyl)phenyl]sulfonylbenzamide) or ABT-737 (4-[4-[[2-(4-chlorophenyl)phenyl]methyl]piperazin-1-yl]-N-[4-[[(2R)-4-(dimethylamino)-1-phenylsulfanylbutan-2-yl]amino]-3-nitrophenyl]sulfonylbenzamide) with dinaciclib potentiated the apoptotic response induced by each single drug. The synergistic killing by ABT-737 with dinaciclib led to cell death accompanied by the hallmarks of apoptosis, including an early loss of the mitochondrial transmembrane potential; the release of cytochrome c, smac/DIABLO, and apoptosis-inducing factor; phosphatidylserine exposure on the plasma membrane surface and activation of caspases and poly ADP-ribose polymerase. Mechanistic studies revealed that dinaciclib promoted proteasomal degradation of Mcl-1. These observations may have important clinical implications for the design of experimental treatment protocols for malignant human glioma.

Introduction

Gliomas are the most common primary tumors in the adult central nervous system. Malignant glioblastoma is characterized by rapid cell proliferation, high invasion, and genetic alterations. Despite advances in all treatment modalities with aggressive surgical resection combined with irradiation and chemotherapy, the median survival remains poor. During malignant transformation, a number of genetic alterations are involved in glioma oncogenesis, including inactivation of tumor suppressor genes such as p16, Rb, p53, and phosphate and tensin homolog on chromosome 10 (PTEN), as well as amplification and overexpression of the cyclin-dependent kinase (CDK) 4 and epidermal growth factor receptor (EGFR) genes (Wen et al., 2006; Bleeker et al., 2012; Bastien et al., 2015). A specific and oncogenic EGFR mutant (EGFRviii) can be detected in about one-third of GBMs (Nishikawa et al., 2004) that activates the RAS/RAF/MEK/MAP kinase, phosphoinositide 3-kinase, mTOR, and STAT pathways to high levels (Tsurushima et al., 1996; Mizoguchi et al., 2006; Akhavan et al., 2010). Disruption of the TP53 and RB

This work was supported by the National Institutes of Health [Grant P01NS40923], by Connor's Cure Foundation Fund, the Translational Brain Tumor Research Fund, and the Scientific Program Fund of the Children's Hospital of Pittsburgh Foundation, and by a grant from Ian's Friends Foundation (all to I.F.P.).
dx.doi.org/10.1124/jpet.115.230052.
[S] This article has supplemental material available at jpet.aspetjournals.org.

ABBREVIATIONS: CDK, cyclin-dependent kinase; DMSO, dimethyl sulfoxide; DSP, dithiobis(succinimidylpropionate); EGFR, epidermal growth factor receptor; FACS, fluorescence-activated cell sorting; MTS, 3-[4,5-dimethylthiazol- 2yl]-5-[3-carboxymethoxyphenyl]-2-[4-sulfophenyl]-2H, tetrazolium; PARP, poly ADP-ribose polymerase; PBS, phosphate-buffered saline; PI, propidium iodide; TBS, Tris-buffered saline; PTEN/MMAC, phosphatase and tensin homolog on chromosome 10/mutated in multiple advanced cancers.

(retinoblastoma) pathways also occurs in gliomas through direct mutation, deletion (Henson et al., 1994; Ohgaki et al., 2004) or amplification of MDM2 (Riemenschneider et al., 1999) or CDK4 (Schmidt et al., 1994), respectively. PTEN is mutated or deleted in 30%–40% of gliomas (Wang et al., 1997), the p53 tumor suppressor gene is mutated or deleted in ~50%, and the Ink4A/Arf locus is also commonly deleted (Ohgaki et al., 2004; Parsons et al., 2008). The cyclin-D/CDK4, CDK6/p16INK4a/pRB/E2F pathway, a key regulator of G1 to S phase transition of the cell cycle, is disrupted in the vast majority of human malignant gliomas and is one of the hallmarks of this tumor type. Common defects include homozygous deletion of CDKN2A/2B (52%), amplification of CDK4 (18%), amplification of CDK6 (1%), and deletion or mutation of RB (12%) (Ohgaki et al., 2004; Parsons et al., 2008; Bastien et al., 2015).

Because many human cancers harbor genetic events that activate CDKs, it has been hypothesized that selective CDK inhibitors may have broad antitumor activity in human malignancies (Asghar et al., 2015). Several CDK inhibitors, including dinaciclib (Merck, Kenilworth, NJ), palbociclib (Pfizer, New York, NY), abemaciclib (Lilly, Southlake, TX), BAY1000394 (Bayer Healthcare, Leverkusen, Germany), and ribociclib (Novartis Pharmaceuticals Corp., Basel, Switzerland) are currently in clinical trials for various advanced cancers (Asghar et al., 2015, Gallorini et al., 2012). Dinaciclib inhibits CDKs 1, 2, 5, and 9 and entered phase 2 and 3 clinical trials in a range of malignancies and displayed tolerable toxicity (Parry et al., 2010; Nemunaitis et al., 2013; Fabre et al., 2014; Asghar et al., 2015, Kumar et al., 2015). Parry et al. (2010) also showed that dinaciclib inhibited cell proliferation and cell-cycle progression in multiple tumor cell lines across a broad range of tumor types with different genetic backgrounds and induced regression of established solid tumors in mouse models. Despite research advances, reports of randomized phase 2 trials of dinaciclib in solid tumors have been disappointing (Mita et al., 2014), with no significant response in patients with non–small cell lung cancer (Stephenson et al., 2014) or acute lymphoblastic leukemia (Gojo et al., 2013). In this study, we investigated the cellular responses to CDK inhibitors in a panel of glioma cancer cell lines. Unlike other CDK inhibitors (e.g., ribociclib, palbociclib, AZD-5438, and AMG-925), dinaciclib produced a dose-dependent reduction of cell proliferation at low nanomolar concentrations in a number of glioma cells with different genetic backgrounds.

ABT -737 is a promising chemotherapeutic agent that promotes apoptosis by acting as a selective BH3 mimetic to neutralize Bcl-2–like family members (Oltersdorf et al., 2005). In preclinical experiments, ABT-737 showed strong antiproliferative and proapoptotic effects in a wide variety of cell types (Bodet et al., 2011). Many cancers, particularly gliomas, are resistant to apoptosis by upregulation of antiapoptotic Bcl-2 family members (Premkumar et al., 2012). One shortcoming with its use is that Mcl-1, a member of the Bcl-2 family, is poorly inhibited by ABT-737 and thus is a major cause of resistance. Because we observed that the effects of this agent were almost entirely cytostatic rather than cytotoxic, we questioned whether the efficacy of dinaciclib could be enhanced by combining it with a second agent that tipped the balance in favor of apoptosis rather than cell-cycle arrest. Because Gojo et al. (2013) demonstrated dinaciclib-induced in vivo inhibition of Mcl-1 expression in patients' peripheral blood mononuclear cells, we hypothesized that combining dinaciclib and ABT-737 would potentiate apoptosis induction in glioma. In this study, we demonstrated the potential benefit of combining the CDK inhibitor dinaciclib with the Bcl-2/Bcl-xL antagonist ABT-737, and here we highlight the potential benefits of simultaneously targeting both survival pathways in patients with glioma.

Materials and Methods

Cell Lines. Established malignant human glioma cell lines such as U373, T98G, A172, and LN229 were obtained from the American Type Culture Collection (Manassas, VA). LN18 and LNZ308 were provided by Dr. Nicolas de Tribolet (Lausanne, Switzerland). The establishment of the parental human glioblastoma cell line, U87 and its derivatives, which overexpress exogenous wild-type EGFR (U87-EGFR-WT), or constitutively active EGFR with a genomic deletion of exons 2–7 (U87-EGFRviii) has been described elsewhere (Huang et al., 1997). The cell lines were kindly provided by Dr. Shi-Yuan Cheng (Northwestern University Feinberg School of Medicine, Chicago, IL). Genetic features (Table 1) of these glioma cell lines have been characterized elsewhere (Furnari et al., 1997; Weller et al., 1998). Cell culture conditions of these cell lines were as previously described (Nagane et al., 1996; Premkumar et al., 2015). Cell lines used in this study were authenticated using short tandem repeat (STR) analysis by ATCC cell line authentication service. The cell line sample was processed using the ABI Prism 3500xl Genetic Analyzer. Data were analyzed using GeneMapper ID-X v1.2 software (Applied Biosystems, Foster City, CA). The genetic profiles for the samples were identical to the reported profile.

Reagents and Antibodies. Dinaciclib, ribociclib, palbociclib, gefitinib, sorafenib, dasatinib, vorinostat, panobinostat, rapamycin, bortezomib, cucurbitacin-I, AZD-6244, YM-155, NVP-AUY922, AMG-925, ABT-737, ABT-263, MK-2206, XL-147, NVP-BKM120, and

TABLE 1
Genotypic features of the glioma cell lines used in this study
IC50 concentrations for CDK inhibitors at 72 hours of treatment as determined by MTS assay.

	Cell Line	Genotypic Features			CDK Inhibitors, IC50 (μM)				
		TP53	PTEN	P14 ARF	Dina	Ribo	Palbo	AZD5438	AMG925
1	U87	Homo, WT/WT	Del	Del	0.024	>20	>20	11.68	4.99
2	LNZ308	Hetero, del/translocated	Del	WT	0.034	>20	>20	2.49	5.86
3	A172	Hetero, WT/WT	Del	Del	0.020	>20	>10	2.93	7.87
4	U373	Homo, Mut273	Mu	WT	0.021	>20	>20	2.59	7.99
5	LN229	Hetero, WT/Mut164	WT	Del	0.041	NT	NT	NT	NT
6	LN18	Hetero, WT/Mut238	WT	Del	0.022	>20	14.08	2.25	5.73
7	T98G	Homo, Mut237	Mut	Del	0.514	>20	>20	14.36	12.33

Del, deleted; Dina, dinaciclib; Hetero, heterozygous; Homo, homozygous; Mut, mutant; NT, not tested; Pablo, palbociclib; Ribo, ribociclib; WT, wild-type.

NVP-BEZ235 were purchased from Chemie Tek (Indianapolis, IN). Enzastaurin, everolimus, WP-1066, AZD-5438, and U0126 were from Selleck (Houston, TX). Chemotherapeutics and all other chemicals used in this study were from Sigma (St. Louis, MO). Unless otherwise indicated, all antibodies were purchased from Cell Signaling Technology (Beverly, MA).

Cell Proliferation Analysis. Cells (5×10^3/well) were plated in 96-well microtiter plates (Costar, Cambridge, MA) in 100 μl of growth medium and, after overnight attachment, exposed for the indicated intervals to inhibitors or vehicle (dimethyl sulfoxide, DMSO). After treatment (72 hours) at 37°C, cells were washed in medium, and the number of viable cells was determined using a colorimetric cell proliferation assay (CellTiter96 Aqueous NonRadioactive Cell Proliferation Assay; Promega, Madison, WI) essentially by incubating cells in the MTS solution for 2 hours and by determining the absorbance at 490-nm wavelength, as reported previously (Jane et al., 2014). IC50 values for the inhibitors were calculated with probit analysis, using IBM SPSS 22 (IBM, Armonk, NY). For growth kinetics analysis (doubling time), 1000 cells were seeded in a 96-well plate with 200 μl of complete growth media and incubated at 37°C, 5% CO_2, for 24, 48, 72, and 96 hours. At each time point, triplicate wells with predetermined cell numbers were subjected to the preceding assay (i.e., MTS cell proliferation assay) in parallel with the test samples. The growth curve was plotted, and the doubling time was calculated from regression equation of the curve as described previously (Premkumar et al., 2006).

Annexin V Apoptosis Assay. Apoptosis induction in vehicle- or inhibitor-treated cells was assayed by the detection of membrane externalization of phosphatidylserine using an Annexin V assay kit (Molecular Probes, Invitrogen, Eugene, OR) as described previously (Jane et al., 2014). 2×10^5 cells were harvested at various intervals after treatment, washed with ice-cold phosphate-buffered saline (PBS), and resuspended in 200 μl of binding buffer. Annexin V-fluorescein isothiocyanate and 1 μg/ml propidium iodide (PI) were added, and cells were incubated for 15 minutes in a dark environment. Labeling was analyzed by flow cytometry with a fluorescence-activated cell sorter FACSCalibur flow cytometer (BD Biosciences, San Jose, CA). Annexin V binds to phosphatidylserine, which translocates from the inner leaflet to the outer leaflet of the plasma membrane in apoptotic cells, so cells that are positive for annexin V staining (i.e., high annexin V signal) are undergoing apoptosis. PI staining provides a measure of cell viability and is used to distinguish between cells in early and late apoptosis (in early apoptosis, PI signal is low; lower right quadrant), and in late apoptosis PI signal is high (upper right quadrant). Cells positive for both annexin-V and PI represent dying cells (upper left quadrant).

Clonogenic Growth Assay. The effect of different inhibitor concentrations on cell viability was also assessed using a clonogenic assay. For this analysis, 250 cells were plated in six-well trays in growth medium, and after overnight attachment, cells were exposed to selected inhibitor concentrations or vehicle for the indicated duration. Cells were then washed with inhibitor-free medium and allowed to grow for 2 weeks under inhibitor-free conditions. Cells were then fixed and stained according to the manufacturer's protocol (Hema 3 Manual Staining Systems; Fisher Scientific, Pittsburgh, PA). After staining, six-well plates were scanned, and images were assembled using Adobe Photoshop CS2 software (Adobe Systems, San Jose, CA).

Combination Index Analysis. Logarithmically growing glioma cells were seeded in 96-well microplates at 5000 cells/well and were allowed to attach overnight. Cells were treated with increasing concentrations of single-agent dinaciclib, ABT-737, or the combination of both in a fixed concentration ratio. Control cells received DMSO. Cell viability was measured using MTS cell proliferation assay as described already herein. The dose-effect curve parameters for both dinaciclib and ABT-737 were used for the calculation of the combination index by the Calcusyn software (BIOSOFT, Cambridge, UK), where combination index values <1, $=1$, and >1 indicate synergism, additivity, and antagonism, respectively (Chou and Talalay 1984).

Cell-Cycle Analysis. The effect of varying concentrations of inhibitors on cell-cycle distribution was determined by flow cytometric analysis of the nuclear DNA content as previously described (Jane et al., 2014). Briefly, cells grown exponentially to 50%–60% confluency were exposed to the inhibitors or DMSO for a range of intervals, harvested, washed in ice-cold PBS, and fixed in 70% ethanol. DNA was stained by incubating the cells in PBS containing PI (50 μg/ml) and RNase A (1 mg/ml) for 60 minutes at room temperature, and fluorescence was measured and analyzed using a Becton Dickinson FACScan and Cell Quest software (Becton Dickinson Immunocytometry Systems, San Jose, CA).

DiOC6 Labeling and Detection of Mitochondrial Membrane Depolarization. Mitochondrial membrane depolarization was measured as described previously (Premkumar et al., 2012; Jane et al., 2013). In brief, floating cells were collected, and attached cells were trypsinized and resuspended in PBS. Cells were loaded with 50 nM 3′,3′-dihexyloxacarbo-cyanine iodide (DiOC6, Molecular Probes, Invitrogen) at 37°C for 15 minutes. The positively charged DiOC6 accumulates in intact mitochondria, whereas mitochondria with depolarized membranes accumulate less DiOC6. Cells were spun at 3000*g*, rinsed with PBS twice, and resuspended in 1 ml of PBS. After the acquisition of data (CellQuest software (Becton Dickinson), the cell fluorescence information was saved in the Flow Cytometry Standard (.fcs) format. These files were then accessed with the FlowJo analysis software (Tree Star, Inc., Ashland, OR). Through this software, the fluorescence data were plotted as histograms, which were converted into and saved as Scalable Vector Graphics (.svg) files. Using Inkscape (The Inkscape Team), an Open Source vector graphics editor, the data were compiled into two-dimensional histogram overlays for comparative analysis. The loss of mitochondrial membrane potential was quantified in FlowJo by gating any left-shifted populations and subtracting from control, and the percentage of cells with decreased fluorescence was determined.

Immunoprecipitation and Western Blotting Analysis. Cells were washed in cold PBS and lysed in buffer containing 30 mM HEPES, 10% glycerol, 1% Triton X-100, 100 mM NaCl, 10 mM $MgCl_2$, 5 mM EDTA, 2 mM Na_3VO_4, 2 mM β-glycerophosphate, 1 mM phenylmethylsulfonyl fluoride, 1 mM 4-(2-aminoethyl) benzenesulfonyl fluoride, 0.8 μM aprotinin, 50 μM bestatin, 15 μM E-64, 20 μM leupeptin, and 10 μM pepstatin A for 15 minutes on ice. Samples were centrifuged at 12,000*g* for 15 minutes, supernatants were isolated, and protein was quantified using Protein Assay Reagent (Pierce Chemical, Rockford, IL). Equal amounts of protein were separated by SDS-PAGE and electrotransferred onto a nylon membrane (Invitrogen). Nonspecific antibody binding was blocked by incubation of the membranes with 4% bovine serum albumin in Tris-buffered saline (TBS)/Tween 20 (0.1%). The membranes were then probed with appropriate dilutions of primary antibody overnight at 4°C. The antibody-labeled blots were washed three times in TBS/Tween 20 and incubated with a 1:2000 dilution of horseradish peroxidase-conjugated secondary antibody in TBS/Tween 20 at room temperature for 1 hour. Proteins were visualized by Western Blot Chemiluminescence Reagent (Cell Signaling). Where indicated, the membranes were reprobed with antibodies against β-actin to ensure equal loading and transfer of proteins.

For Bax immunoprecipitation, cell extracts were prepared by lysing 5×10^6 cells on ice for 30 minutes in CHAPS lysis buffer (10 mM HEPES (pH 7.4), 150 mM NaCl, 1% CHAPS, protease, phosphatase inhibitors). Lysates were clarified by centrifugation at 15,000*g* for 10 minutes at 4°C, and the protein concentrations in the supernatants were determined. Equal amounts of protein extracts were incubated overnight with primary antibody (active Bax, 6A7, Sigma). Afterward, Dynabeads Protein G (Invitrogen) was added for 2 hours, followed by magnetic separation of the immunoprecipitated fraction; Western blot analysis was carried out as described already herein.

Subcellular Fractionation. Cells were treated with or without inhibitors, and cytosolic proteins were fractionated as described previously (Premkumar et al., 2013). Briefly, cells were resuspended

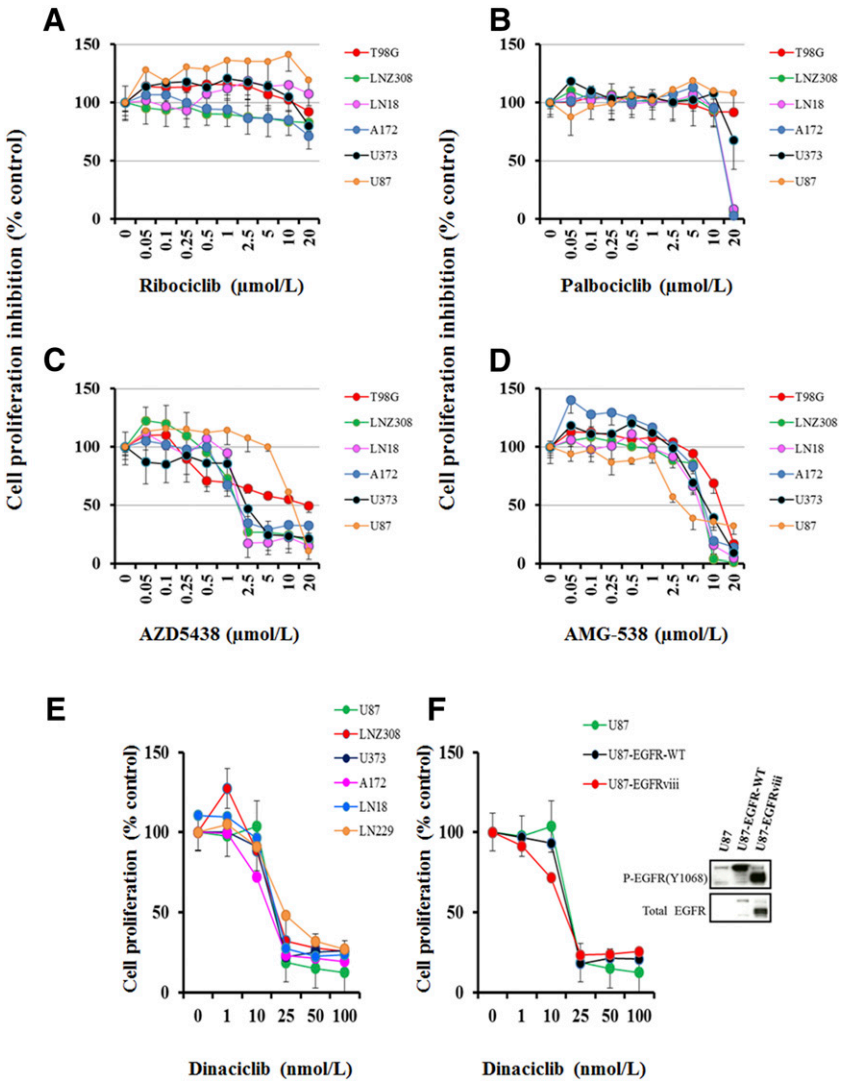

Fig. 1. Differential response to CDK inhibitors in malignant human glioma cell lines. Established malignant human glioma cell lines were grown on 96-well plates in growth medium and, after an overnight attachment period, were exposed to selected concentrations of ribociclib (A), palbociclib (B), AZD-5438 (C), AMG-925 (D), or dinaciclib (E). Control cells received vehicle (DMSO, 0) for 72 hours. Cell proliferation inhibition was assessed semiquantitatively by spectrophotometric measurement of MTS bioreduction. Points represent the mean of three measurements carried out in triplicate. (F) Equal amounts of protein from logarithmically growing EGFR-overexpressing cell lines U87-EGFR-WT, U87-EGFRviii, and isogenic control U87 were separated by SDS-PAGE analysis and subjected to Western blotting analysis with the indicated primary antibodies (F, right panel). In parallel, cell proliferation assay was performed with dinaciclib as described in *Materials and Methods* (F, left panel). Points represent the mean of three measurements ± S.D.

in a lysis buffer containing 0.025% digitonin, sucrose (250 mM), HEPES (20 mM, pH 7.4), $MgCl_2$ (5 mM), KCl (10 mM), EDTA (1 mM), phenylmethylsulfonyl fluoride (1 mM), 10 μg/ml aprotinin, and 10 μg/ml leupeptin. After 10-minute incubation at 4°C, cells were centrifuged (2 minutes at 13,000*g*), and the supernatant (cytosolic fraction) was removed and frozen at −80 ° C for subsequent use.

In Vitro Cross-Linking and Analysis of Bax Oligomerization. Cytosolic and membrane fractions were prepared by selective plasma membrane permeabilization with 0.05% digitonin, followed by membrane solubilization with 1% CHAPS as described elsewhere (Premkumar et al., 2012). Briefly, control and experimental cells in dishes were treated with 0.05% digitonin in isotonic buffer (10 mM HEPES, 150 mM NaCl, 1.5 mM $MgCl_2$, 1 mM EGTA, pH 7.4) containing protease inhibitors [1 mM 4-(2-aminoethyl) benzenesulfonyl fluoride hydrochloride, 0.8 mM aprotinin, 50 mM bestatin, 15 mM E-64, 20 mM leupeptin, 10 mM pepstatin A], for 1 or 2 minutes at room temperature. The permeabilized cells were shifted to 4°C, scraped with a rubber policeman, and collected into centrifuge tubes. The supernatants (digitonin-extracted cytosolic fraction) were routinely collected after centrifugation at 15,000*g* for 10 minutes. After centrifugation, the pellet was washed with isotonic buffer and further extracted with ice-cold detergent (1% CHAPS) in isotonic buffer containing protease inhibitors for 60 minutes at 4°C to release membrane- and organelle bound proteins, including mitochondrial cytochrome c. The CHAPS soluble membrane fractions were collected by high speed (15,000*g*) centrifugation for 10 minutes. Protein cross-linker, DSP [dithiobis(succinimidylpropionate)] was dissolved in DMSO and prepared just before use. Equal amounts of CHAPS-extracted membrane fraction protein were incubated with 1 mM DSP for 45 minutes at room temperature and subsequently quenched by adding 20 mM Tris-HCl (pH 7.4). Proteins were resolved by nonreducing SDS-PAGE, and immunoblots were analyzed as described herein.

Transient Transfection. Optimal 29mer-pRS-shRNA constructs were obtained from OriGene (Rockville, MD). Sequences specific for human Mcl-1 and nontarget control shRNA sequences were used for this study. Cells were seeded in six-well plates and allowed to reach 70%–80% confluence. Transfection of targeting or control (nontargeting) shRNA was performed by using FuGene 6 according to the manufacturer's recommendations (Roche Applied Science, Indianapolis, IN). One microgram of shRNA in 100 μl Opti-MEM medium was mixed with 2 μl of FuGene 6. After the mixture was incubated at room temperature for 20 minutes, complete medium was added to make the total volume up to 2 ml. For overexpression studies, cells were transfected with 2.0 μg of MCL-1 expression plasmid (catalog number RC200521, OriGene) or control vector, pCMV-6 (catalog number PS100001, OriGene) as described herein. After 48 hours, medium was changed and cells were incubated with inhibitors for 24 hours. Cell viability (annexin V/PI binding) or Western blot analysis was carried out as described herein.

Fluorescence Microscopy. Cells were grown on chamber slides (Nalge Nunc, Naperville, IL) in growth medium and, after an

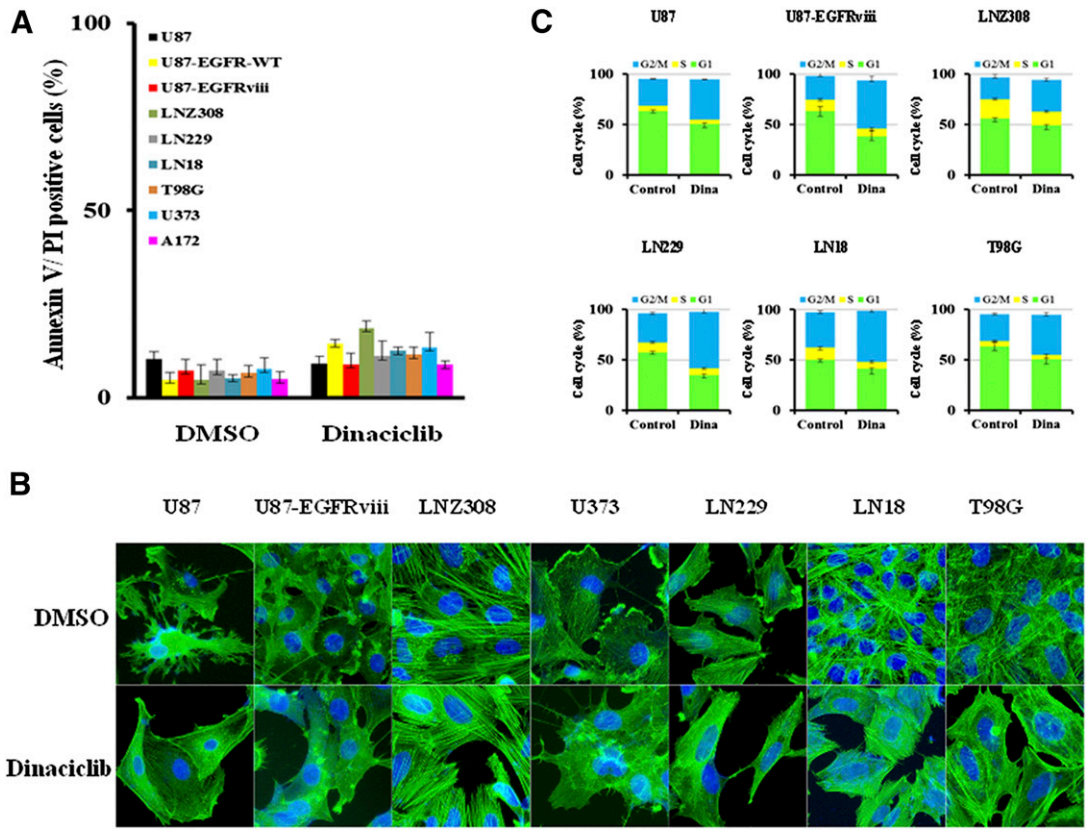

Fig. 2. Cytostatic effect of dinaciclib on in vitro cultured glioma cells (A) U87, U87-EGFR-WT, U87-EGFRviii, LNZ308, LN229, LN18, T98G, U373, and A172 cells were seeded at 60% confluence, allowed to attach overnight, and treated with dinaciclib (5.0 μM) for 24 hours. Control cells received an equivalent amount of DMSO. Apoptosis was analyzed by flow cytometry. Bar chart represents data from three independent experiments. (B) U87, U87-EGFRviii, LNZ308, U373, LN229, LN18, and A172 cells were seeded at 60% confluence, allowed to attach overnight, and treated with dinaciclib (2.5 μM) for 24 hours. Cells were stained with Alexa Flour 488 Phalloidin as described in *Materials and Methods*. Nuclei were stained with DAPI. Control cells received DMSO. Morphologic and nuclear changes in response to inhibitor treatment were evaluated by microscopic inspection. (C) U87, U87-EGFRviii, LNZ308, U373, LN229, LN18, and A172 cells were seeded at 60% confluence, allowed to attach overnight, and treated with dinaciclib (2.5 μM) for 24 hours. Cell-cycle analysis using PI staining was performed as described in *Materials and Methods*. Results represent the mean of three independent experiments.

overnight attachment period, were exposed to selected concentrations of inhibitor or vehicle (DMSO). Cells were washed once with PBS, fixed with 3.7% formaldehyde for 30 minutes, and stained with Alexa Fluor 488 Phalloidin (Thermo Fisher Scientific, 1:200 dilutions) and DAPI (1:1000) for 2 hours at room temperature. The slides were then washed in PBS, mounted, and examined under a fluorescent microscope. Morphologic changes in response to inhibitor treatment were evaluated by microscopic (EVOS, Thermo Fisher Scientific) inspection.

Statistical Analysis. Unless otherwise stated, data are expressed as mean ± S.D. The significance of differences between experimental conditions was determined using a two-tailed Student's t test. Differences were considered significant at $P < 0.05$.

Results

Differential Response to CDK Inhibitors in Malignant Human Glioma Cell Lines. In this study, we assessed the antiproliferative activity of CDK inhibitors ribociclib, palbociclib, AZD-5348, AMG-935, and dinaciclib in a panel of glioma cell lines representing a range of genetic features (Table 1). Cells were treated with increasing concentrations of inhibitors for 72 hours, and MTS assay was performed as described in *Materials and Methods*. No significant growth inhibition was seen after 72 hours of treatment with as high as 15–20 μM ribociclib (Fig. 1A) and palbociclib (Fig. 1B). The IC50 (inhibitory concentration of 50%) for AZD5438 (Fig. 1C) and AMG-925 (Fig. 1D) ranged between 2 and 15 μM and 5 and 12 μM, respectively (Table 1); however, glioma cells were very sensitive to dinaciclib. The IC50 ranged between 20 and 40 nM on day 3 of culture (Fig. 1E; Table 1), suggesting that dinaciclib was the most potent agent among all tested CDK inhibitors in glioma. Interestingly, although most of the glioma cell lines showed exquisite sensitivity to dinaciclib, a degree of resistance was seen in T98G cell lines (IC50 > 500 nM; Table 1).

Alterations of the epidermal growth factor receptor (EGFR) gene are common in glioma. This prompted us to test the effect of dinaciclib in EGFR overexpressing cell lines. We used isogenic U87 cell lines expressing U87-EGFR-WT and U87-EGFRviii (Fig. 1F, Western blot). As shown in Fig. 1F, dinaciclib caused concentration-dependent inhibition of cell proliferation, the IC50 ranging between 10 and 20 nM, regardless of EGFR amplification status. No correlation was found between the sensitivity of cells to dinaciclib and the doubling time (Supplemental Table 1). Taken together, our results suggest that dinaciclib is a potent inhibitor, and the sensitivity does not appear to correlate with p53, $p14^{ARF}$, and PTEN or EGFR amplification status of human glioma cell lines.

Cytostatic Effect of Dinaciclib on In Vitro Cultured Glioma Cells. To quantify the effects on apoptosis, U87,

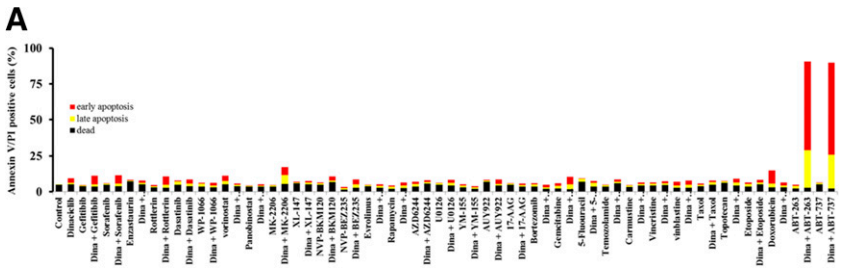

Fig. 3. Combined treatment with dinaciclib and ABT-737 effectively kills glioma cells. (A) T98G cells were seeded at 60% confluence, allowed to attach overnight, and treated with dinaciclib (1.0 μM) or indicated signaling inhibitor (refer to Supplemental Table 2 for the concentrations used in this study) or the combination of both for 24 hours. Control cells received an equivalent amount of DMSO. Apoptosis was analyzed by flow cytometry as described in *Materials and Methods*. The results represent the mean of two independent experiments representing various stages of cell death. (B) U87, U87-EGFRviii, LNZ308, LN229, LN18, and T98G cells were treated with dinaciclib (100 nM (D), ABT-737 (100 nM) (A), or the combination of both (D and A). Control cells received DMSO (C). Apoptosis was analyzed by flow cytometry as described in *Materials and Methods*. The results represent the mean of three independent experiments. (C) In parallel, cell extracts (from U87, LNZ308, and T98G) were prepared, and equal amounts of protein were separated by SDS-PAGE and subjected to Western blot analysis with the indicated antibodies. β-actin served as loading control. The results of a representative study are shown; two additional experiments produced similar results.

U87-EGFR-WT, U87-EGFRviii, LNZ308, A172, U373, LN18, LN229, and T98G cells were treated with dinaciclib for 24 hours, stained with annexin V and PI, and analyzed by flow cytometry. Our results reveal that more than ~85% of glioma cells treated with amounts as high as 5.0μM dinaciclib were negative for both PI and annexin V and thus were viable (Fig. 2A). A representative FACS histogram is shown in Supplemental Fig. 1. We also examined the cellular and nuclear morphology after phalloidin and Hoechst staining. As shown in Fig. 2B, cells treated with 2.5μM dinaciclib for 24 hours exhibited no significant cellular or nuclear changes (characteristic features of apoptosis such as nuclear condensation/fragmentation and morphology changes such as cell shrinkage, membrane blebbing). Cell-cycle analysis by flow cytometry further revealed that dinaciclib induced cell-cycle arrest at the G2/M phase of the cell cycle, in which the cell fraction increased by 20%–30% to 45%–55% at 24 hours, whereas the G1 phase fraction decreased (Fig. 2C). Then we used colony-forming assays to determine whether inhibitor-treated cells divide and reenter the cell cycle and retain their capacity for long-term cell survival and proliferation. As shown in the Supplemental Fig. 2A, the short-term presence of dinaciclib (24-hour exposure with inhibitor followed by 14 days growth in inhibitor-free media) produced a concentration-dependent reduction of viable colonies compared with DMSO-treated control cells. Interestingly, the long-term presence of dinaciclib (72-hour exposure with inhibitor followed by 14 days growth in inhibitor-free media) showed a significant inhibition of colony size (Supplemental Fig. 2B) but did not induce cell death (data not shown).

Combined Treatment with Dinaciclib and ABT-737 Effectively Kills Glioma Cells. Because clinically achievable concentrations of dinaciclib (82.3–184 nM) inhibited proliferation but failed to induce apoptosis in glioma (Fig. 2A), we examined a panel of agents that could potentially be combined with dinaciclib to promote tumor cell killing. We selected this panel of inhibitors to represent a spectrum of mechanisms that might promote apoptosis, including receptor kinase inhibitors (gefitinib and sorafenib), PKC inhibitors (enzastaurin and rottlerin), Src family kinase inhibitor (dasatinib), JAK/STAT inhibitor (WP-1066), histone deacetylase inhibitors (vorinostat and panobinostat), phosphatidylinositol 3-kinase/Akt/mTOR pathway inhibitors (MK2206, XL-147, NVP-BKM120, NVP-BEZ235, everolimus, and rapamycin), MAP kinase inhibitors (AZD6244 and UO126), survivin inhibitor (YM-155), heat-shock protein inhibitors (NVP-AUY922 and 17-AAG), proteasomal inhibitor (bortezomib), Bcl-2/Bcl-xL inhibitors (ABT-737 and ABT-263), and chemotherapeutic agents (DNA strand termination, gemcitabine and 5-fluouracil; DNA alkylation, temozolomide and carmustine; disruption of microtubule dynamics, vincristine, vinblastine and taxol; topoisomerase- II inhibition, topotecan, etoposide and doxorubicin), for their effect on cell viability. For most agents, we did not observe a clear annexin V/PI-positive population of cells treated with the inhibitors alone or in combination with dinaciclib; however, coadministration of dinaciclib and ABT-263 or dinaciclib and ABT-737 significantly increased annexin V + and PI + cells (Fig. 3A; Supplemental Table 2). Then we performed combination index dose-effect isobologram analysis as described in *Materials and Methods*. The combination of dinaciclib with ABT-737 produced a synergistic inhibition (Fig. 3B; Supplemental Table 3), suggesting that the cotreatment of dinaciclib plus ABT-737 has the potential not only to increase the rate of treatment response but also to reduce the concentration of each inhibitor needed to elicit a given effect. In parallel, whole cell lysates were examined by Western blot analysis. It is important to note that at as great a concentration as 10.0 μM, dinaciclib as a single agent does not activate or cleave the 32-kDa procaspase-3 into a -p20, -p17, or -p12-kDa "active" form, nor was poly ADP-ribose polymerase (PARP) cleaved to form a 89-kDa fragment); however, simultaneous treatment with dinaciclib (at clinically achievable concentrations, 25–100 nM) plus ABT-737 (100 nM) resulted in the appearance of cleaved fragments of caspase 3 and PARP and induction of cell death, suggesting the involvement of caspase-dependent pathways (Fig. 3C) and the greater benefit in combination than evidenced by either single agent alone. Likewise, It is apparent that dinaciclib (100 nM) or ABT-737 (100 nM) minimally inhibited the formation of colonies; in contrast, cultures exposed to the combination of ABT-737 and dinaciclib completely abolished colony-forming ability, suggesting the chemotherapeutic potential of these inhibitors in combination against glioma (Supplemental Fig. 2A).

Effect of Dinaciclib and ABT-737 on the Cell-Cycle Profile and the Expression Levels of Cell-Cycle Regulatory Proteins. To elucidate the molecular mechanisms

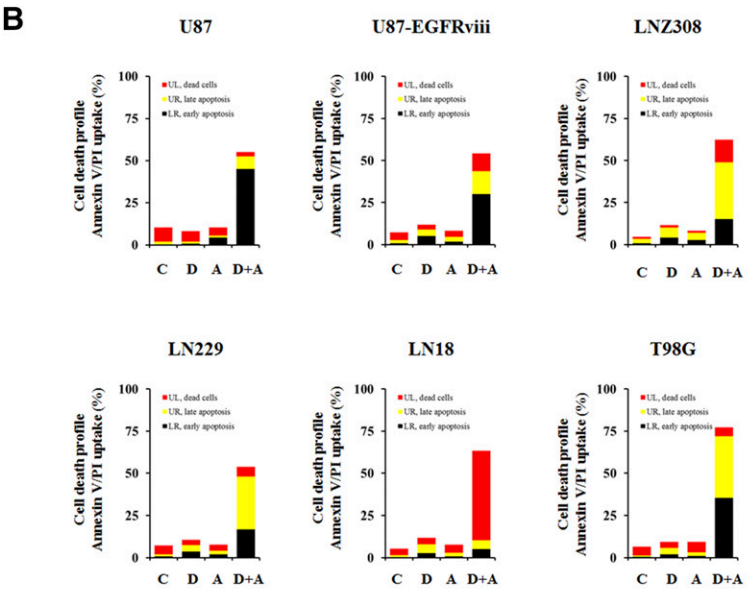

Fig. 3. Continued

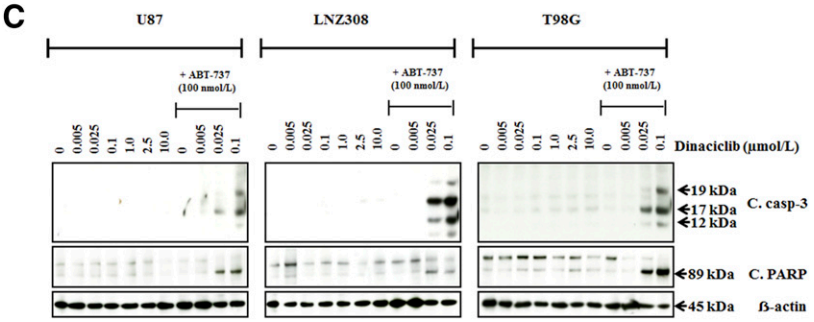

underlying this biologic effect, we examined the alteration in cell-cycle regulatory protein expression on dinaciclib treatment in U87, U87-EGFRviii, LNZ308, LN229, LN18, and T98G glioma cell lines. No correlation was found between the sensitivity of cells to dinaciclib and the expression of cell-cycle regulatory proteins. As shown in Fig. 4A, low levels of CDK2 and CDK 6 expression were seen in LNZ308 and U87 cell lines. Dinaciclib did not significantly alter CDK1, CDK2, CDK4, CDK6, and CDK7 expression levels (Fig. 4A). In contrast, treatment of glioma cells with different concentrations of dinaciclib for 24 hours resulted in a concentration-dependent reduction of CDK9, cyclin B1, cyclin D1, and cyclin D3 protein expression compared with the DMSO-treated cells. Expression levels of the CDK inhibitor p21, but not p27, was decreased prominently (data not shown). Phosphorylation status of Rb, which participates directly in the control of cell cycle, was also examined. As shown in Fig. 4B, dinaciclib downregulated phosphorylation of RB, whereas total Rb levels were unchanged.

Because downregulation of Mcl-1 has been observed to confer sensitivity to ABT-737 and our annexin V/PI studies in this report (Fig. 3, A and B) suggest that ABT-737 can, in principle, increase the sensitivity of glioma cells to dinaciclib, we examined Bcl-2 family proteins by Western blot analysis. The expression level of Mcl-1 was markedly downregulated in all glioma cell lines (Fig. 4B), whereas that of Bcl-2, Bcl-xL, Bid, Bcl-w, Bim, and Bak were unchanged (data not shown). Of note, ABT-737 as a single agent (100 nM) or in combination with dinaciclib (indicated concentrations) did not significantly alter the expression levels of cell-cycle regulatory proteins (Fig. 4A).

Cotreatment with Dinaciclib and ABT-737 Induces Mitochondrial Membrane Potential Dysfunction and Conformational Changes of the Proapoptotic Protein Bax. Because Bcl-2 family proteins are key regulators of the mitochondrial apoptotic pathway and changes in mitochondrial membrane potential ($\Delta\psi$m) are thought to represent an early event in the induction of apoptosis and likely capture the effects of agents on various aspects of Bcl-2 family member homeostasis, we evaluated the effect of ABT-737 with or without dinaciclib on $\Delta\psi$m. The integrity of the mitochondrial membranes of the cells was examined by DiOC6 staining and flow cytometry; the decrease in fluorescence intensity reflected the loss of $\Delta\psi$m. DiOC6 enters the mitochondria in healthy cells but leaches into the cytosol of the cell on $\Delta\psi$m dissipation, resulting in decreased fluorescence intensity. Uncoupling of mitochondrial respiration with CCCP served as a positive control (data not shown). U87, U87-EGFRviii, LNZ308, LN229, LN18, and T98G cells treated with varying concentrations of dinaciclib and the loss of mitochondrial membrane potential were analyzed as described in *Materials and Methods*. A representative FACS plot (Fig. 5, A–C) and a

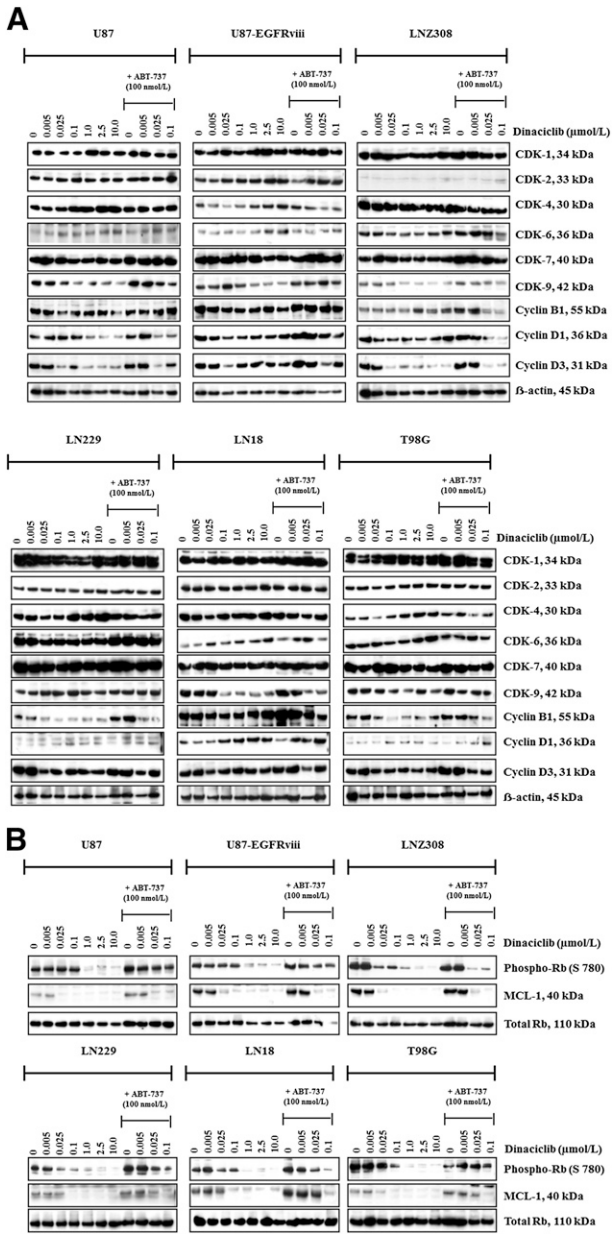

Fig. 4. Effect of dinaciclib and ABT-737 on the cell-cycle profile and the expression levels of cell-cycle regulatory proteins. (A and B) Logarithmically growing U87, U87-EGFRviii, LNZ308 (upper panel), LN229, LN18, and T98G (lower panel) cells were treated with dinaciclib (indicated concentrations) or ABT-737 (100 nM) or the combination of both for 24 hours. Control cells received equivalent concentrations of vehicle, DMSO. Whole-cell extracts were prepared, and equal amounts of protein were separated by SDS-PAGE and subjected to Western blotting analysis with the indicated antibodies. β-actin served as loading control (A). Total Rb served as loading control (B). The results of a representative study are shown; two additional experiments produced similar results.

histogram obtained from multiple experiments are shown in Supplemental Fig. 3. Levels as high as 1.0 μM of dinaciclib or ABT-737 individually resulted in a minimal or no decrease in fluorescence intensity (Fig. 5, A and B, respectively). By contrast, coadministration of dinaciclib (25 nM) and ABT-737 (50 nM) enhanced the loss of mitochondrial membrane potential (Fig. 5C, appearance of a population to the left). Pretreatment with the pan-caspase inhibitor zVAD-fmk partially reversed the $\triangle\psi$m, suggesting that dinaciclib and ABT-737-induced cell death is associated with damage to the mitochondrial membrane (data not shown). Because cytochrome c release from mitochondria is an early, pivotal event in the apoptosis of many cell types, cytosolic fractions of cell lysates were analyzed by immunoblotting for cytochrome c, smac/DIABLO, and apoptosis-inducing factor. Cotreatment with dinaciclib and ABT-737 strongly increased the release of mitochondrial apoptogenic factors, cytochrome c, apoptosis-inducing factor, and smac/DIABLO in the cytoplasmic fraction compared with cells treated with single agents (Fig. 5D).

Bax and Bak are generally believed to be responsible for mitochondrial outer membrane permeabilization initiating the release of caspase activators such as cytochrome c, which is a key step in the events leading to the eventual cell death. The release of cytochrome c into the cytosol prompted us to analyze the involvement of upstream regulators of mitochondrial membrane perturbations, such as Bax and Bak. To investigate Bax and Bak involvement, we used Bax (6A7, monoclonal Bax antibody, Sigma) and Bak antibodies (1-Ab, monoclonal Bak antibody; Calbiochem) that recognize the active conformations of the respective proteins. Immunoprecipitation followed by Western blot analysis, was performed as described in *Materials and Methods*. Western blotting showed an increase in the amount of activated Bax in glioma cells treated with dinaciclib and ABT-737 for various times. No Bak activation was evident in glioma cell lines (data not shown). In contrast, there was no activation of Bax in cells treated with each agent individually (Fig. 5E).

Homo-oligomerization of Bax has been hypothesized to be responsible for cell death through the mitochondria-dependent apoptosis pathway. To address the effect of dinaciclib and ABT-737, we examined Bax homo-oligomerization in glioma cell lines. Freshly prepared mitochondrial membrane fractions from untreated or treated cells were incubated with DSP (dithiobissuccinimidyl propionate), a membrane-permeable homo-bifunctional amine-reactive cross-linking agent. As shown in Fig. 5F, cross-linked Bax protein complexes were observed in U87, U87-EGFRviii, LNZ308, LN229, LN18, and T98G cells.

Dinaciclib Promotes Proteasomal Degradation of Mcl-1 and Enhances ABT-737-Mediated Cell Death in Malignant Human Glioma Cell Lines. Because Mcl-1 protein expression is regulated by multiple mechanisms, including degradation by the proteasome, we examined whether Mcl-1 protein stability was affected by exposure to dinaciclib. Cells were cultured in dinaciclib with or without proteasomal inhibitor MG132 for the indicated duration. Western blot analysis (Fig. 6A), indicated that the decrease in Mcl-1 protein levels was inhibited in the proteasome-suppressed (MG132 treated) cells, indicating the involvement of proteasomal degradation of Mcl-1. Furthermore, consistent with our previous studies (Jane et al., 2013), shRNA-mediated knockdown of Mcl-1 significantly promoted ABT-737-induced cell death compared with nontarget shRNA (Fig. 6B). To further validate the requirement for Mcl-1 in the synergistic killing activity of dinaciclib plus ABT-737, cells were transfected with Mcl-1, treated with dinaciclib or ABT-737 alone or in combination. Western blotting of total cell lysates indicated overall expression levels of Mcl-1 protein levels. Annexin V/propidium analysis of cells containing the empty expression vector displayed high levels of cell death in the presence of

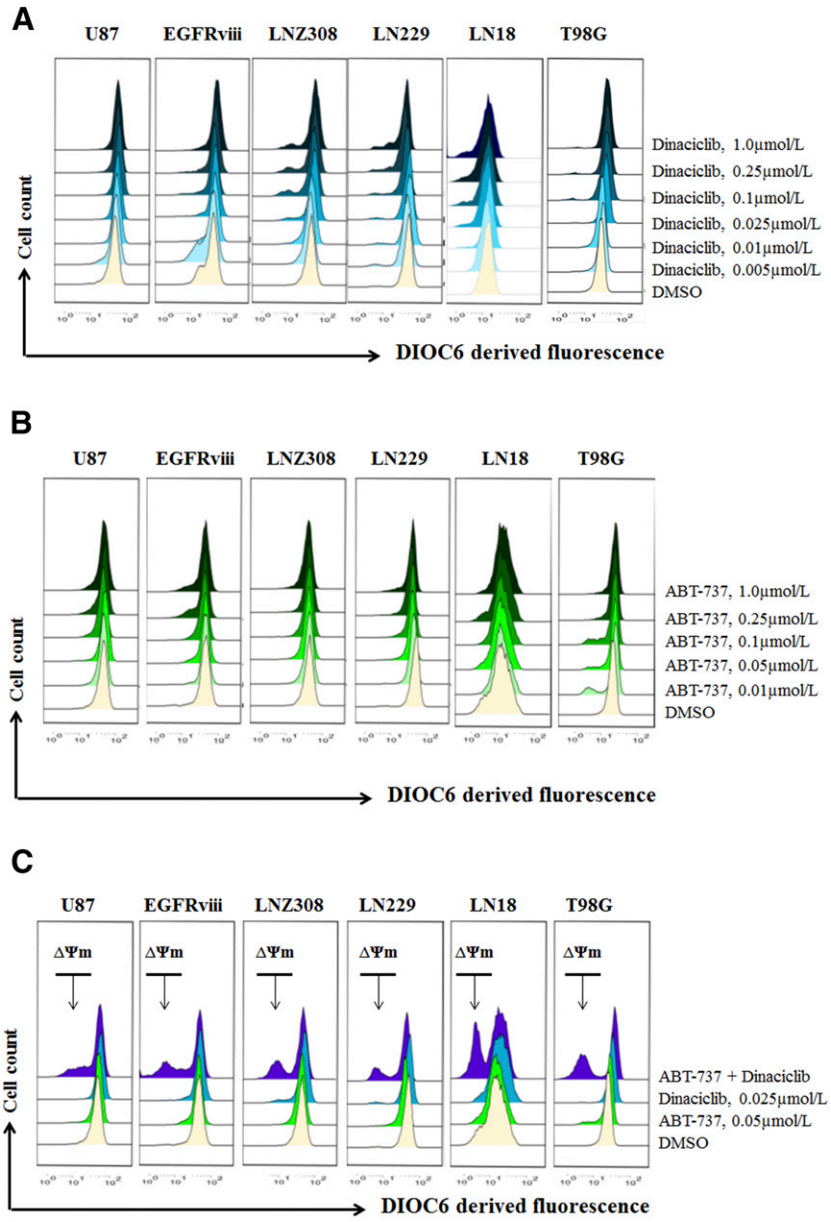

Fig. 5. Cotreatment with dinaciclib and ABT-737 induces mitochondrial membrane potential dysfunction and conformational changes of the proapoptotic protein Bax. Logarithmically growing U87, U87-EGFRviii, LNZ308, LN229, LN18, and T98G cells were treated with dinaciclib (indicated concentrations) (A), ABT-737 (indicated concentrations (B), or the combination of both (indicated concentrations (C) for 24 hours. The integrity of the mitochondrial membranes of the cells was examined by DiOC6 staining and flow cytometry. (D) U87, U87-EGFRviii, LNZ308, LN229, LN18, and T98G cells were treated with dinaciclib (50 nM) or ABT-737 (50 nM) or the combination of both for indicated durations. Cytosolic extracts were prepared, and equal amounts of protein were separated by SDS-PAGE and subjected to Western blotting analysis with the indicated antibodies. (E), U87, U87-EGFRviii, LNZ308, LN229, LN18, and T98G cells were treated with dinaciclib (50 nM) or ABT-737 (50 nmol/L) or the combination of both for the indicated duration and lysed with 1% CHAPS buffer. An equal amount of protein (500 μg) was immunoprecipitated with monoclonal anti-Bax (6A7; Sigma-Aldrich) antibody and then subjected to Western blot analysis with polyclonal anti-Bax antibody (Cell Signaling Technology). (F) U87, U87-EGFRviii, LNZ308, LN229, LN18, and T98G cells were treated with dinaciclib (50 nM) or ABT-737 (50 nM) or the combination of both for 12 hours. Control cells received equivalent amounts of DMSO. Membrane fractions were obtained as described in *Materials and Methods*, and proportional amounts corresponding to total protein were analyzed for Bax oligomerization by Western blotting under nonreducing conditions. Slow-moving Bax oligomers in DSP cross-linked cells were derived from Bax monomers, and the molecular masses of oligomers containing Bax were calculated by plotting their migrations against migrations of molecular mass standards (left panel, mol. wt. marker). The results of a representative study are shown; two additional experiments produced similar results.

both dinaciclib and ABT-737; whereas cells overexpressing Mcl-1 were more resistant to cell death induced by the drug combination (Fig. 6C), suggesting a protective role of Mcl-1 in preventing cell death induced by the combination of dinaciclib and ABT-737.

Discussion

It is clear that genetic alterations in malignant gliomas affect cell proliferation and cell-cycle control, which are the targets of most chemotherapeutic agents (small molecules and antibodies); however, early clinical data from the use of CDK inhibitors are largely disappointing. Dinaciclib is a novel CDK1, CDK2, CDK5, and CDK9 inhibitor that inhibits cell proliferation and induces apoptosis in a variety of human cell lines. Compared with flavopiridol, dinaciclib showed a superior therapeutic index in a preclinical setting (Parry et al., 2010). Preliminary pharmacokinetic data from clinical studies in solid tumors suggest that average dinaciclib concentrations of 82.3–184 nM can be achieved (Mita et al., 2014; Gojo et al., 2013). Using a large panel of glioma cell lines, we have demonstrated that CDK inhibitors effectively inhibit cell proliferation. Our data, however, suggest that concentrations in this clinically achievable range cause growth inhibition, but not killing, of glioma cells (Fig. 2, A and B and Fig. 3, A–C), which is consistent with the observation that with the exception of CLL and osteosarcoma (Lin et al., 2009; Phelps et al., 2009; Fu et al., 2011), single-agent CDK inhibitors have demonstrated only modest clinical anticancer activity in a broad range of tumors, suggesting the need for combining CDK inhibitors with chemotherapy or other novel signaling inhibitors to provide an effective response (Cicenas and Valius, 2011).

In this study, dinaciclib was screened in combination with clinical or experimental cancer therapeutics. A unique synergistic activity was observed when dinaciclib was combined with ABT-737 or ABT-263, small-molecule Bcl-2/Bcl-xL antagonists. Previously, using a panel of glioma cell lines, we

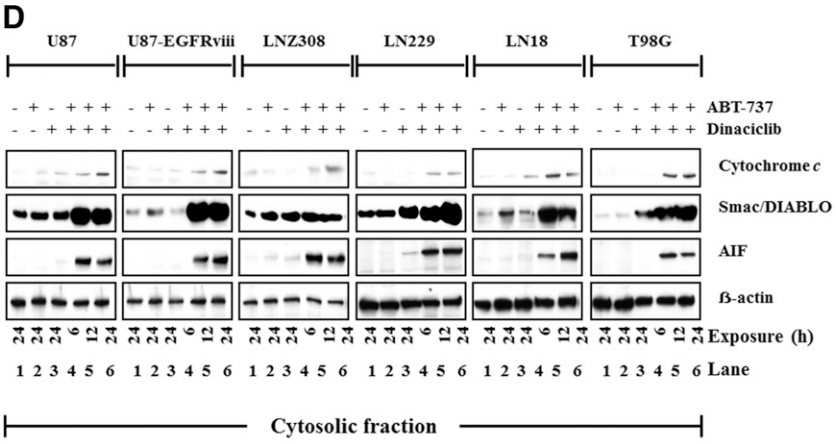

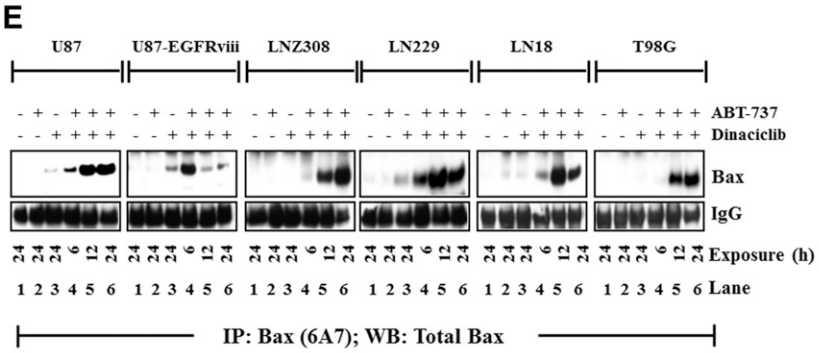

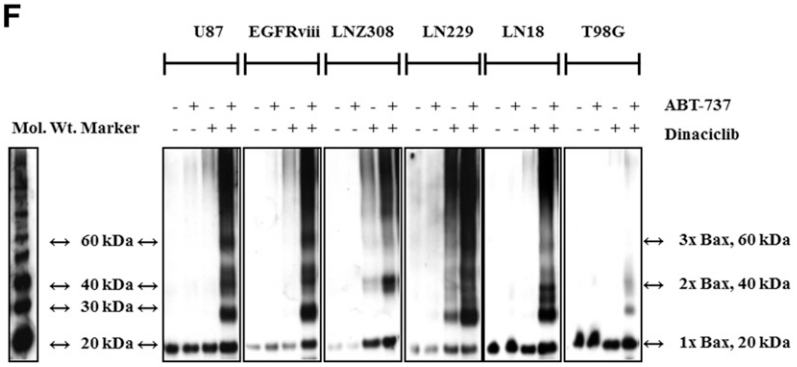

Fig. 5. Continued

have demonstrated that malignant human glioma cells are resistant to ABT-737, with an IC50 around 30–50 μM after 24 hours of exposure (Premkumar et al., 2012). Interestingly, as shown in Fig. 3B, when low nanomolar concentrations of dinaciclib were combined with ABT-737, a detectable synergistic effect in killing by apoptotic activation was evidenced, regardless of p53/PTEN/EGFR/p14^{ARF} status.

From a molecular standpoint, a logical interpretation of data presented on the ability of ABT-737 to synergistically induce apoptosis in glioma cells when combined with dinaciclib reflects the possibility that these two signaling inhibitors simultaneously modulate multiple regulatory pathways with key areas of interactions. We have demonstrated that dinaciclib inhibits Rb phosphorylation and the expression levels of Mcl-1 in a concentration-dependent manner. These effects were seen at pharmacologically relevant concentrations. It has been established by us (Jane et al., 2013) and others (Konopleva et al., 2006; van Delft et al., 2006; Chen et al., 2007) that pharmacological or genetic depletion of Mcl-1 sensitizes tumor cells to ABT-737. In this study, we have shown the ability of dinaciclib to downregulate Mcl-1, which may represent a critical event in mediating the synergism with ABT-737 in killing glioma cells. This effect is likely occurring at the post-translational level by acting on enzymes regulating Mcl-1 half-life. With a very short half-life, Mcl-1 expression is regulated at multiple levels. It has been previously shown that more than six protein kinases, five E3 ubiquitin-ligases, and one deubiquitinase and ubiquitin-independent proteasomal degradation are involved in the regulation of Mcl-1 stability (Mojsa et al., 2014). Here, we have demonstrated that dinaciclib modulated Mcl-1 expression through promoting proteasome-mediated degradation; however, the relative contributions of the other mechanisms were not examined in this study. Our results showed that the

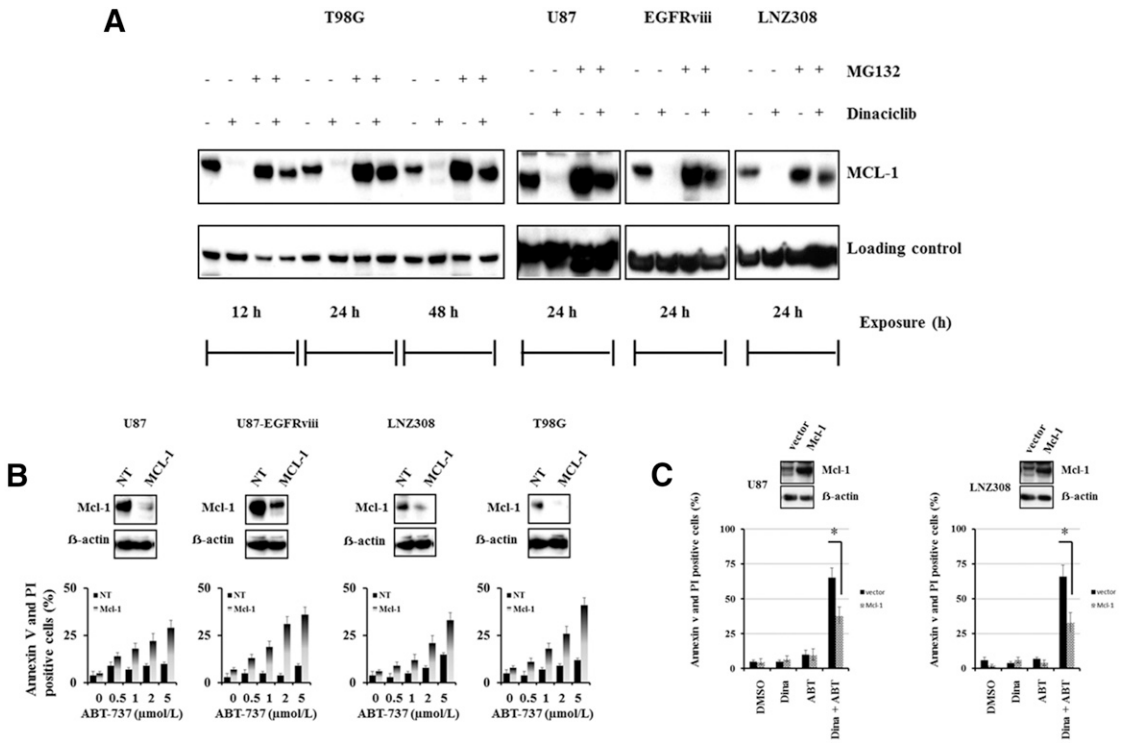

Fig. 6. Dinaciclib promotes proteasomal degradation of Mcl-1 and enhances ABT-737-mediated cell death in malignant human glioma cell lines. (A) Logarithmically growing T98G, U87, U87-EGFRviii, and LNZ308 cells were pretreated with 1.0 μM of MG-132 (proteasomal inhibitor) for 2 hours followed by dinaciclib (250 nM) for the indicated duration. Cell extracts were subjected to Western blot analysis with the indicated antibody. β-actin served as loading control. (B) U87, U87-EGFRviii, LNZ308, and T98G cells were transfected with nontarget (NT) or Mcl-1 shRNA as described in *Materials and Methods*. Forty-eight hours post-transfection, cells were treated with the indicated concentrations of ABT-737 for 24 hours, and viability was assessed by annexin V/PI apoptosis assay (lower panel). In parallel, cell lysates were collected and protein was subjected to Western blot analysis using Mcl-1 antibody. Immunoblots were stripped and reprobed with β-actin. (C) U87 and LNZ308 cells were transfected with vector (pCMV) or Mcl-1 expression vector as described in *Materials and Methods*. Forty-eight hours post-transfection, cells were treated with dinaciclib (dina, 100 nM) or ABT-737 (ABT, 100 nM) or the combination of both (dina + ABT) for 24 hours, and viability was assessed by annexin V/PI apoptosis assay (lower panel). In parallel, cell lysates were collected, and protein was subjected to Western blot analysis using Mcl-1 antibody. Immunoblots were stripped and reprobed with β-actin. Data are representative of triplicate studies from three independent experiments. $^*P < 0.005$.

downregulation of Mcl-1 occurred without any significant change in Mcl-1 mRNA levels (data not shown).

Combined treatment with dinaciclib and ABT-737 induced the loss of mitochondrial membrane potential, activated the mitochondrial pathway of apoptosis in glioma, as evidenced by cleavage of caspase-3 and PARP (caspase-9, data not shown) and accumulation of cytosolic cytochrome c, smac/DIABLO, apoptosis-inducing factor, and activation of Bax. The activation of Bax, including Bax conformational changes and oligomerization, appears to play a crucial role in the initiation of dinaciclib- and ABT-737-induced apoptosis, consistent with our observation that the activation of Bax, including Bax conformational changes and oligomerization, appears to play an important role in the initiation of apoptosis after targeted therapies in gliomas (Premkumar et al., 2012; Foster et al., 2014). Annis et al. (2005) presented evidence that Bax inserts into the mitochondrial outer membrane as a monomer and then undergoes a conformational change and homo-oligomerization to form pores. When we used single agents in the same concentrations as in the combination therapies, neither dinaciclib nor ABT-737 was associated with any significant change in $\Delta\psi$m or induction of apoptosis. The combination of dinaciclib and ABT-737 strongly induced mitochondrial membrane depolarization, as shown by flow cytometry with DiOC6 dye and subsequent potent induction of apoptosis as shown by annexin V/PI analysis, suggesting that pharmacologic interaction of these agents enhances the mitochondrial outer membrane permeabilization, followed by effective conformational activation and oligomerization of Bax.

Although clinical trials showed that dinaciclib displayed tolerable toxicity (Parry et al., 2010; Nemunaitis et al., 2013; Fabre et al., 2014; Asghar et al., 2015; Kumar et al., 2015), some reports of randomized phase 2 trials of dinaciclib have been disappointing (Mita et al., 2014) with no significant response, particularly in patients with non–small cell lung cancer (Stephenson et al., 2014) or acute lymphoblastic leukemia (Gojo et al., 2013). In this study, we showed that neither ABT-737 nor dinaciclib is a potent cytotoxic agent when used alone and that efficacy was poor at the clinically achievable range. In contrast, the combination of dinaciclib plus ABT-737 at clinically achievable concentrations readily sensitized glioma cells to apoptosis induction by downregulating Mcl-1, regardless of EGFR/PTEN/p53/p14ARF status. The combination of dinaciclib and ABT-737 activated the mitochondrial pathway of apoptosis in glioma cell lines in a caspase-dependent manner. We also demonstrated that Bax, a major proapoptotic effector, undergoes conformational changes and seems to play a crucial role in the initiation of dinaciclib-plus-ABT-737–induced cell death. Regarding the mechanisms, treatment with dinaciclib promotes proteasomal degradation of Mcl-1 and significantly enhanced ABT-737 sensitivity. Because Mcl-1 protein is associated with early

tumor recurrence and shorter survival in glioma patients (Rieger et al., 1998), combining dinaciclib with ABT-737 is a promising strategy to overcome the multiple nonoverlapping resistance mechanisms that characterize these highly aggressive tumors.

Acknowledgments

The authors thank Alexis Styche for fluorescence-activated cell sorter analysis.

Authorship Contributions

Participated in research design: Premkumar, Pollack.

Conducted experiments: Jane, Premkumar, Cavaleri, Sutera, Rajasekar.

Contributed new reagents or analytic tools: Jane, Premkumar.

Performed data analysis: Jane, Premkumar, Cavaleri, Sutera, Rajasekar, Pollack.

Wrote or contributed to the writing of the manuscript: Premkumar, Pollack.

References

Akhavan D, Cloughesy TF, and Mischel PS (2010) mTOR signaling in glioblastoma: lessons learned from bench to bedside. *Neuro-oncol* **12**:882–889.

Annis MG, Soucie EL, Dlugosz PJ, Cruz-Aguado JA, Penn LZ, Leber B, and Andrews DW (2005) Bax forms multispanning monomers that oligomerize to permeabilize membranes during apoptosis. *EMBO J* **24**:2096–2103.

Asghar U, Witkiewicz AK, Turner NC, and Knudsen ES (2015) The history and future of targeting cyclin-dependent kinases in cancer therapy. *Nat Rev Drug Discov* **14**:130–146.

Bastien JI, McNeill KA, and Fine HA (2015) Molecular characterizations of glioblastoma, targeted therapy, and clinical results to date. *Cancer* **121**:502–516.

Bleeker FE, Molenaar RJ, and Leenstra S (2012) Recent advances in the molecular understanding of glioblastoma. *J Neurooncol* **108**:11–27.

Bodet L, Gomez-Bougie P, Touzeau C, Dousset C, Descamps G, Maïga S, Avet-Loiseau H, Bataille R, Moreau P, and Le Gouill S, et al. (2011) ABT-737 is highly effective against molecular subgroups of multiple myeloma. *Blood* **118**:3901–3910.

Chen S, Dai Y, Harada H, Dent P, and Grant S (2007) Mcl-1 down-regulation potentiates ABT-737 lethality by cooperatively inducing Bak activation and Bax translocation. *Cancer Res* **67**:782–791.

Chou TC and Talalay P (1984) Quantitative analysis of dose-effect relationships: the combined effects of multiple drugs or enzyme inhibitors. *Adv Enzyme Regul* **22**:27–55.

Cicenas J and Valius M (2011) The CDK inhibitors in cancer research and therapy. *J Cancer Res Clin Oncol* **137**:1409–1418.

Fabre C, Gobbi M, Ezzili C, Zoubir M, Sablin MP, Small K, Im E, Shinwari N, Zhang D, and Zhou H, et al. (2014) Clinical study of the novel cyclin-dependent kinase inhibitor dinaciclib in combination with rituximab in relapsed/refractory chronic lymphocytic leukemia patients. *Cancer Chemother Pharmacol* **74**:1057–1064.

Foster KA, Jane EP, Premkumar DR, Morales A, and Pollack IF (2014) Coadministration of ABT-737 and SAHA induces apoptosis, mediated by Noxa upregulation, Bax activation and mitochondrial dysfunction in PTEN-intact malignant human glioma cell lines. *J Neurooncol* **120**:459–472.

Fu W, Ma L, Chu B, Wang X, Bui MM, Gemmer J, Altiok S, and Pledger WJ (2011) The cyclin-dependent kinase inhibitor SCH 727965 (dinacliclib) induces the apoptosis of osteosarcoma cells. *Mol Cancer Ther* **10**:1018–1027.

Furnari FB, Lin H, Huang HS, and Cavenee WK (1997) Growth suppression of glioma cells by PTEN requires a functional phosphatase catalytic domain. *Proc Natl Acad Sci USA* **94**:12479–12484.

Gallorini M, Cataldi A, and di Giacomo V (2012) Cyclin-dependent kinase modulators and cancer therapy. *BioDrugs* **26**:377–391.

Gojo I, Sadowska M, Walker A, Feldman EJ, Iyer SP, Baer MR, Sausville EA, Lapidus RG, Zhang D, and Zhu Y, et al. (2013) Clinical and laboratory studies of the novel cyclin-dependent kinase inhibitor dinaciclib (SCH 727965) in acute leukemias. *Cancer Chemother Pharmacol* **72**:897–908.

Henson JW, Schnitker BL, Correa KM, von Deimling A, Fassbender F, Xu HJ, Benedict WF, Yandell DW, and Louis DN (1994) The retinoblastoma gene is involved in malignant progression of astrocytomas. *Ann Neurol* **36**:714–721.

Huang HS, Nagane M, Klingbeil CK, Lin H, Nishikawa R, Ji XD, Huang CM, Gill GN, Wiley HS, and Cavenee WK (1997) The enhanced tumorigenic activity of a mutant epidermal growth factor receptor common in human cancers is mediated by threshold levels of constitutive tyrosine phosphorylation and unattenuated signaling. *J Biol Chem* **272**:2927–2935.

Jane EP, Premkumar DR, DiDomenico JD, Hu B, Cheng SY, and Pollack IF (2013) YM-155 potentiates the effect of ABT-737 in malignant human glioma cells via survivin and Mcl-1 downregulation in an EGFR-dependent context. *Mol Cancer Ther* **12**:326–338.

Jane EP, Premkumar DR, Morales A, Foster KA, and Pollack IF (2014) Inhibition of phosphatidylinositol 3-kinase/AKT signaling by NVP-BKM120 promotes ABT-737-induced toxicity in a caspase-dependent manner through mitochondrial dysfunction and DNA damage response in established and primary cultured glioblastoma cells. *J Pharmacol Exp Ther* **350**:22–35.

Konopleva M, Contractor R, Tsao T, Samudio I, Ruvolo PP, Kitada S, Deng X, Zhai D, Shi YX, and Sneed T, et al. (2006) Mechanisms of apoptosis sensitivity and resistance to the BH3 mimetic ABT-737 in acute myeloid leukemia. *Cancer Cell* **10**:375–388.

Kumar SK, LaPlant B, Chng WJ, Zonder J, Callander N, Fonseca R, Fruth B, Roy V, Erlichman C, and Stewart AK; Mayo Phase 2 Consortium (2015) Dinaciclib, a novel CDK inhibitor, demonstrates encouraging single-agent activity in patients with relapsed multiple myeloma. *Blood* **125**:443–448.

Lin TS, Ruppert AS, Johnson AJ, Fischer B, Heerema NA, Andritsos LA, Blum KA, Flynn JM, Jones JA, and Hu W, et al. (2009) Phase II study of flavopiridol in relapsed chronic lymphocytic leukemia demonstrating high response rates in genetically high-risk disease. *J Clin Oncol* **27**:6012–6018.

Mita MM, Joy AA, Mita A, Sankhala K, Jou YM, Zhang D, Statkevich P, Zhu Y, Yao SL, and Small K, et al. (2014) Randomized phase II trial of the cyclin-dependent kinase inhibitor dinaciclib (MK-7965) versus capecitabine in patients with advanced breast cancer. *Clin Breast Cancer* **14**:169–176.

Mizoguchi M, Betensky RA, Batchelor TT, Bernay DC, Louis DN, and Nutt CL (2006) Activation of STAT3, MAPK, and AKT in malignant astrocytic gliomas: correlation with EGFR status, tumor grade, and survival. *J Neuropathol Exp Neurol* **65**:1181–1188.

Mojsa B, Lassot I, and Desagher S (2014) Mcl-1 ubiquitination: unique regulation of an essential survival protein. *Cells* **3**:418–437.

Nagane M, Coufal F, Lin H, Bögler O, Cavenee WK, and Huang HJ (1996) A common mutant epidermal growth factor receptor confers enhanced tumorigenicity on human glioblastoma cells by increasing proliferation and reducing apoptosis. *Cancer Res* **56**:5079–5086.

Nemunaitis JJ, Small KA, Kirschmeier P, Zhang D, Zhu Y, Jou YM, Statkevich P, Yao SL, and Bannerji R (2013) A first-in-human, phase 1, dose-escalation study of dinaciclib, a novel cyclin-dependent kinase inhibitor, administered weekly in subjects with advanced malignancies. *J Transl Med* **11**:259–273.

Nishikawa R, Sugiyama T, Narita Y, Furnari F, Cavenee WK, and Matsutani M (2004) Immunohistochemical analysis of the mutant epidermal growth factor, deltaEGFR, in glioblastoma. *Brain Tumor Pathol* **21**:53–56.

Ohgaki H, Dessen P, Jourde B, Horstmann S, Nishikawa T, Di Patre PL, Burkhard C, Schüler D, Probst-Hensch NM, and Maiorka PC, et al. (2004) Genetic pathways to glioblastoma: a population-based study. *Cancer Res* **64**:6892–6899.

Oltersdorf T, Elmore SW, Shoemaker AR, Armstrong RC, Augeri DJ, Belli BA, Bruncko M, Deckwerth TL, Dinges J, and Hajduk PJ, et al. (2005) An inhibitor of Bcl-2 family proteins induces regression of solid tumours. *Nature* **435**:677–681.

Parry D, Guzi T, Shanahan F, Davis N, Prabhavalkar D, Wiswell D, Seghezzi W, Paruch K, Dwyer MP, and Doll R, et al. (2010) Dinaciclib (SCH 727965), a novel and potent cyclin-dependent kinase inhibitor. *Mol Cancer Ther* **9**:2344–2353.

Parsons DW, Jones S, Zhang X, Lin JC, Leary RJ, Angenendt P, Mankoo P, Carter H, Siu IM, and Gallia GL, et al. (2008) An integrated genomic analysis of human glioblastoma multiforme. *Science* **321**:1807–1812.

Phelps MA, Lin TS, Johnson AJ, Hurh E, Rozewski DM, Farley KL, Wu D, Blum KA, Fischer B, and Mitchell SM, et al. (2009) Clinical response and pharmacokinetics from a phase 1 study of an active dosing schedule of flavopiridol in relapsed chronic lymphocytic leukemia. *Blood* **113**:2637–2645.

Premkumar DR, Arnold B, and Pollack IF (2006) Cooperative inhibitory effect of ZD1839 (Iressa) in combination with 17-AAG on glioma cell growth. *Mol Carcinog* **45**:288–301.

Premkumar DR, Jane EP, Agostino NR, DiDomenico JD, and Pollack IF (2013) Bortezomib-induced sensitization of malignant human glioma cells to vorinostat-induced apoptosis depends on reactive oxygen species production, mitochondrial dysfunction, Noxa upregulation, Mcl-1 cleavage, and DNA damage. *Mol Carcinog* **52**:118–133.

Premkumar DR, Jane EP, DiDomenico JD, Vukmer NA, Agostino NR, and Pollack IF (2012) ABT-737 synergizes with bortezomib to induce apoptosis, mediated by Bid cleavage, Bax activation, and mitochondrial dysfunction in an Akt-dependent context in malignant human glioma cell lines. *J Pharmacol Exp Ther* **341**:859–872.

Premkumar DR, Jane EP, and Pollack IF (2015) Cucurbitacin-I inhibits Aurora kinase A, Aurora kinase B and survivin, induces defects in cell cycle progression and promotes ABT-737-induced cell death in a caspase-independent manner in malignant human glioma cells. *Cancer Biol Ther* **16**:233–243.

Rieger L, Weller M, Bornemann A, Schabet M, Dichgans J, and Meyermann R (1998) BCL-2 family protein expression in human malignant glioma: a clinical-pathological correlative study. *J Neurol Sci* **155**:68–75.

Riemenschneider MJ, Büschges R, Wolter M, Reifenberger J, Boström J, Kraus JA, Schlegel U, and Reifenberger G (1999) Amplification and overexpression of the MDM4 (MDMX) gene from 1q32 in a subset of malignant gliomas without TP53 mutation or MDM2 amplification. *Cancer Res* **59**:6091–6096.

Schmidt EE, Ichimura K, Reifenberger G, and Collins VP (1994) CDKN2 (p16/MTS1) gene deletion or CDK4 amplification occurs in the majority of glioblastomas. *Cancer Res* **54**:6321–6324.

Stephenson JJ, Nemunaitis J, Joy AA, Martin JC, Jou YM, Zhang D, Statkevich P, Yao SL, Zhu Y, and Zhou H, et al. (2014) Randomized phase 2 study of the cyclin-dependent kinase inhibitor dinaciclib (MK-7965) versus erlotinib in patients with non-small cell lung cancer. *Lung Cancer* **83**:219–223.

Tsurushima H, Tsuboi K, Yoshii Y, Ohno T, Meguro K, and Nose T (1996) Expression of N-ras gene in gliomas. *Neurol Med Chir (Tokyo)* **36**:704–708.

van Delft MF, Wei AH, Mason KD, Vandenberg CJ, Chen L, Czabotar PE, Willis SN, Scott CL, Day CL, and Cory S, et al. (2006) The BH3 mimetic ABT-737 targets selective Bcl-2 proteins and efficiently induces apoptosis via Bak/Bax if Mcl-1 is neutralized. *Cancer Cell* **10**:389–399.

Wang SI, Puc J, Li J, Bruce JN, Cairns P, Sidransky D, and Parsons R (1997) Somatic mutations of PTEN in glioblastoma multiforme. *Cancer Res* **57**:4183–4186.

Weller M, Rieger J, Grimmel C, Van Meir EG, De Tribolet N, Krajewski S, Reed JC, von Deimling A, and Dichgans J (1998) Predicting chemoresistance in human malignant glioma cells: the role of molecular genetic analyses. *Int J Cancer* **79**:640–644.

Wen PY, Kesari S, and Drappatz J (2006) Malignant gliomas: strategies to increase the effectiveness of targeted molecular treatment. *Expert Rev Anticancer Ther* **6**:733–754.

Address correspondence to: Dr. Daniel R. Premkumar or Dr. Ian F. Pollack, Department of Neurosurgery, Children's Hospital of Pittsburgh, 4401 Penn Avenue, Pittsburgh, PA 15224. E-mail: daniel.premkumar@chp.edu or ian.pollack@chp.edu